Fatigue of Closed Cell Foams

Dan Zenkert[1], Andrey Shipsha and Magnus Burman
Department of Aeronautical and Vehicle Engineering
Kungliga Tekniska Högskolan (KTH)
SE – 100 44 Stockholm, Sweden

Keywords: Cellular materials, foam, fatigue, crack propagation

Abstract

Static properties of foams scale with relative density and this scaling can be obtained through various static tests. The same scaling appears to be valid for both crack propagation rates and fatigue properties of the foams. The implication of this is that once the fatigue behaviour of one relative density foam is established, one can predict the fatigue behaviour of all other density foams within the same class of materials. This paper deals with fatigue of closed cell foams. The main idea is to use a few simple tests to predict the tension-tension fatigue properties of foams. The required testing consists of crack propagation rate measurements and one tension-tension fatigue test performed at yield stress of the foam. This data can then be combined to construct a synthetic S-N curve for the foam. Testing is performed on three densities of Divinycell H-grade and three densities of Rohacell WF-grade foam. A very simple fatigue model, based on an initial flaw approach, is used to link the crack propagation rate behaviour of these foams with their un-notched fatigue life. This approach is backed up by the experimental results. The obtained results can be used to form some general conclusions about the fatigue of closed foams, at least of the types used herein.

Introduction

Rigid cellular foams are extensively used as a structural core in load carrying sandwich structures. The usage stretches over applications in aerospace, automotive, marine, transportation and infra structure. There are numerous examples of applications and a few worth noticing here are for example the new Swedish Navy Corvette Visby, wind-mill blades, and novel train car structures. In all of these and most other foam core sandwich applications, the core is typically a closed cell polymer foam, designed to carry a substantial part of the load. More and more has been focused on the core material recently due to increased demands for material properties and models to use in the design of sandwich structures. Fracture and fatigue of load carrying foam cores still remains to a large extent unknown. The reason for this is the inherent structure of foams, constituted of a complicated 3-dimensional network of thin membranes (cell walls), enclosing each cell. At the intersection of cell walls, edges with concentrated mass build up rods or beams. A foam is not just a material, but also a micro-structure – homogeneous continuum or heterogeneous cell structure, depending on the scale of interest. The macroscopic properties of this structure (material) depend on not only the properties of the material building up these walls and edges but also the microstructure. One important property is of course the relative density, $\overline{\rho}$, defined as the ratio of the density of the foam ρ divided by the density of the solid material ρ_s. The cell structure itself will also

[1] Corresponding author, danz@kth.se

strongly affect the macroscopic properties of the foam. Yet another important parameter is the distribution of solid material that builds up the cell walls and edges, respectively.

In the well-known textbook by Gibson and Ashby [1] cellular foams (3D cellular structure materials) are modelled using a simplified geometrical model. A variety of properties are then predicted using the relative density, the properties of the solid cell edge/face material and the cell structure. Rather straight forward kinematic relations are used and very useful, simple formulae for design are derived. In essence, most properties of foams can be written as

$$\bar{x} = \alpha \bar{\rho}^{n} \tag{1}$$

where x is some mechanical property of the foam normalised with its value for the fully dense material (bulk property) of which the cell edges and faces are made of, in the case of polymer foams thus the solid polymer material property.

In the derivation of foam properties, a distinction must be made between open and closed cell foams; open cell foams are made up of small beams or struts (edges) connected to each other. A closed cell foam is on the other hand made of a number of plate like membranes (faces) connected at their edges forming closed cells. The deformation mechanism in open cell foams is bending of the edges while in closed cell foams the dominating deformation mechanism rather should be cell face stretching. Gibson and Ashby [1] derives that the Young's modulus scale with the square of the relative density for open cell foams and linearly for closed cell foams. Similar relations are also derived for the strength giving a relative density scaling varying between $n = 1$ and $n = 2$. Another issue is that the ratio between the material in edges and walls is usually unknown and hard to measure, so any clear distinction will be uncertain. One important issue to discuss herein is that the models for fracture toughness of foams, as given in [1] assumes that cracks in foams grow stepwise, one cell at the time. This implies that the relations found for the fracture toughness will be a function of the cell size of the foam.

Herein, we shall assume that the mechanical properties of the foam can be described by means of eq.(1), where the exponent n will be found from fitting experimental data. However, this exponent must have a value $1 \leq n \leq 2$.

Very little have been reported on fatigue of foams. Some early work was performed by Burman *et al* [2-4] on the fatigue of foam core sandwich beams. The fatigue testing in that case was set up so that the foam failed in fatigue and the loading of the foam was primarily in shear. The findings of these studies were that the loading ratio has a large influence on the fatigue life and also that fatigue crack nucleation appears over large volumes in the test specimen before any macroscopic cracks are formed. Similar type of tests has also been performed by others, e.g. Shenoi *et al* [5], Buene *et al* [6] and Kanny and Mahfuz [7]. Kanny and Mahfuz [8] performed fatigue tests of PVC foams in three-point bending and concluded that the fatigue strength increases with relative density. In a subsequent investigation Kulkarni *et al* [9] used sandwich beams in three-point bending and also tried to follow the crack propagation rate in the core once a macroscopic crack had formed. However, the measurement of crack propagation rates was not pursued. McCullough *et al* [10] tested aluminium foams in both tension-tension and compression-compression fatigue. They scale properties of these foams with a power law relation of the type given in eq.(1) with an exponent equal to 1.5. Although the results are not given in terms of a Basquins' law it is found that the slope of the S-N curve is considerably lower in the compression-compression fatigue case. It was also found that high density and low density foams appear to have very

similar S-N curves, though with different amplitude. They also argue that the fatigue degradation mechanism is not due to cracking events in the foam but rather progressive accumulation of strain by material ratchetting analogous to creep. Once the accumulated strain equals the monotonic yield strain the rate of accumulation increases at least one order of magnitude. This leads to the formation of a complete crush band in compression or a rupture band in tension. This is supported also by the fact that the fatigue life is found to be notch insensitive for the metal foams used in their work. Harte *et al* [11] performed fatigue testing of an open and a closed cell aluminium foam. One main outcome of this research is that the fatigue limit of foams appears to be same for all density foams in terms of the ratio of maximum stress in the load cycle to the plastic (yield) stress or the peak tensile stress. The endurance limit in tension is found to be the same for both the open and closed cell foams and approximately equal to the endurance limit of fully dense aluminium. Olurin *et al* [12] performed crack propagation measurement on two closed cell aluminium foams. There are two main conclusions from this work; the first being that the exponent in Paris' law is extremely high, in the order of 20-25, and secondly that the crack propagation mechanism appears to be the degradation of crack bridging of cell edges behind the crack tip. In short, cell walls fail first leaving individual edges bridging the crack flanks. Shipsha *et al* [13,14] used both compact tension (CT) and cracked sandwich beams specimens to measure crack propagation rates in foams and found also high crack propagation rates for polymer foams. They also found that the crack propagation rates were reduced when forcing cracks in foams to grow along an interface in Mode II. Huang and Lin [15] analysed crack propagation data of various density phenolic foams reported in [1] and were able to normalise the Paris' law data to one single generic relation for all density phenolic foams. Of all these reports on fatigue and crack propagation, Huang and Lin [15] present the only framework for linking such data. We will present a similar framework but one that is conceptually different and which is not based on micromechanics.

Materials

Two high performance, rigid polymer foams with closed cell structure were used in this study; Divinycell H-grade and Rohacell WF-grade. Micrographs of the cell structure for these foams are shown in Fig.1.

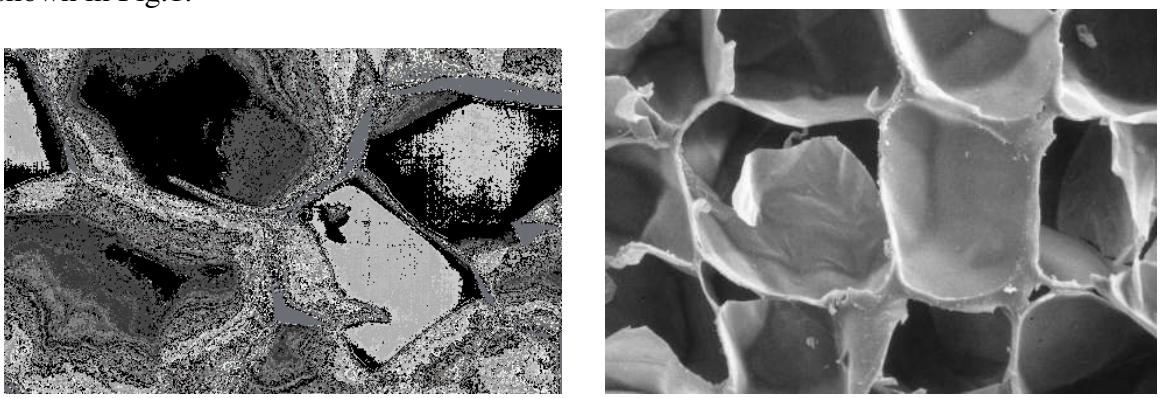

Figure 1 Cell structure of WF51 and H100. Reprinted with permission of Röhm GmbH and DIAB

Divinycell is a cross-linked rigid cellular PVC foam and it is produced in a variety of densities where mechanical properties (higher strength and moduli) increase with density.

Divinycell qualities used in this survey were H60, H100 and H200, where H stands for the grade and the number corresponds to the nominal density in kg/m^3. Any details on this material can be found in [16]. We have herein used a solid density of the cell wall/edge material of 1250 kg/m^3.
The other material used in this study is Rohacell, a PMI foam with predominantly closed cells and which is more brittle than the PVC foam. The qualities used herein were WF51, WF110 and WF200, where WF is the particular grade of Rohacell and the number corresponds to the nominal density in kg/m^3. The solid material density is approximately 1200 kg/m^3. Details on this material can be found [17].
The reason for choosing these two materials is that one exhibits a fairly brittle behaviour (Rohacell) in the context of foams and the other (Divinycell) has a more ductile behaviour (higher strain to failure, a more pronounced plastic regime). Both materials are close to being isotropic, with only small variations in moduli and strengths in the in-plane and out-of-plane directions. As seen from Fig.1, both foams have similar micro-structure. There is a portion of material concentration at the edges, the junctions were the cell walls meet. One could assume that these materials then should have properties somewhere in between what could be expected for perfectly open och closed foams. By fitting handbook data for the materials [16,17] (elastic modulus, ultimate tensile and compressive strength, shear strength, and fracture toughness) the slope n in eq.(1) varies between 1.1 and 1.2 for all static mechanical properties. The data produced from these sources are based on various testing methods.

Static properties

The static tests of foams were preformed using the same test up as in the tension-tension fatigue testing, which is described below. Fig.2a shows tensile stress-strain curves for all materials. From the tensile testing a value of n = 1.1 gives a quite good curve fit to all tensile properties for both materials. Then, taking the stress-strain relations for the materials as obtained in Fig.2a, the same curves are plotted again in Fig.2b, where the stress is normalised with the relative ratio so that $\bar{\sigma} = \sigma / \bar{\rho}^n$ using n = 1.1. As seen in Fig.2b, the three stress-strain responses for three different relative densities collide into a single curve.

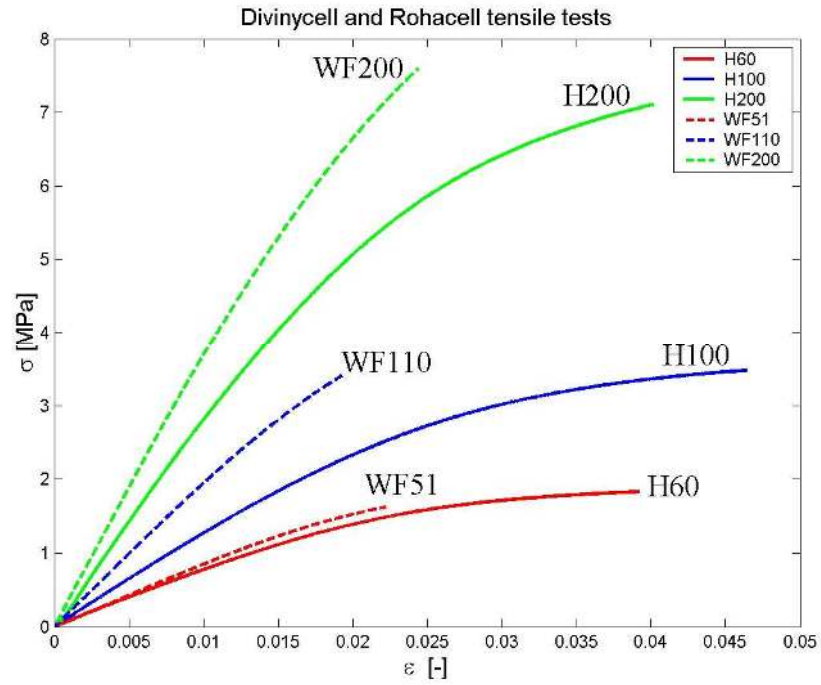

(a)

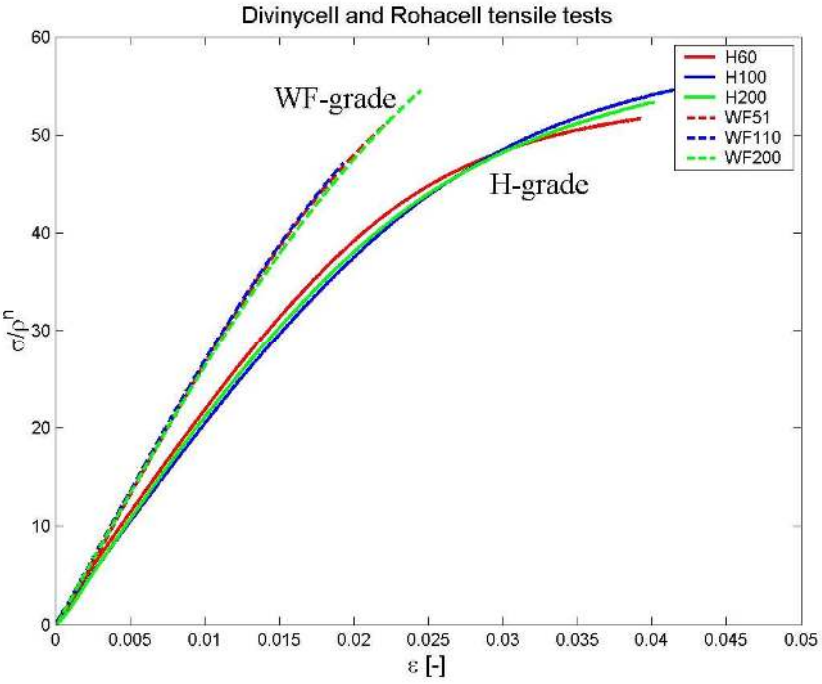

(b)

Figure 2 (a) Typical stress-strain relations for H60, H100 and H200 (solid lines) and WF51, WF110 and WF200 (dashed lines) and (b) normalised stress-strain relations.

From this testing, all the necessary material characteristics used in this investigation can be extracted, including the Young's modulus, E, and the yield stress here defined as the stress at 0.2% offset strain, $\sigma_{0.2}$. The yield stress will be used as a governing tensile parameter for the

fatigue testing, the reason being twofold: First of all, the yield strength ought to be the primary design allowable using these materials, as it is with other types of materials exhibiting some degree of ductility, like metals. This is not always the case in the sandwich structure design community and the common practice is rather to use the ultimate strength as the design allowable. However, this practice appears to be criticized lately. The second reason is that a yield strength defined on the basis of an offset strength is clear and straightforward to define and exhibits low scatter in testing. The material data for the considered materials are given in Table 1.

	H60	H100	H200	WF51	WF110	WF200
E [MPa]	78	126	304	89	206	395
$E/(\bar{\rho})^n \cdot 10^3$	2.01	1.83	2.28	2.81	2.79	2.83
$\sigma_{0.2}$ [MPa]	1.31	2.37	4.61	1.48	3.33	6.43
$\sigma_{0.2}/(\bar{\rho})^n$	33.9	34.3	34.6	46.7	46.1	46.2
σ_{ult} [MPa]	1.86	3.34	7.14	1.60	3.41	7.39
$\sigma_{ult}/(\bar{\rho})^n$	48.1	48.4	53.6	50.5	47.2	53.0
K_{1c} [MPa$\sqrt{\text{m}}$]	0.13	0.21	0.41	0.10	0.19	0.34
$K_{1c}/(\bar{\rho})^n$	3.25	3.04	3.00	2.53	2.60	2.44
C [*]	8.04E3	1.88E2	5.08	1.455E14	1.535E9	1.111E6
m	6	6	6	13	13	13
$C \cdot (\bar{\rho})^{n \times m}$	2.7E-8	2.0E-8	2.8E-8	4.8E-9	4.4E-9	8.3E-9
a_0 [mm] (assuming $f = 1$)	0.20	0.22	0.18	0.30	0.36	0.28

Table 1 Material data for Divinycell H and Rohacell WF materials (* dimension obtained using *da/dN* in mm/cycle in eq.(2))

Fracture toughness tests were performed using a standard cracked four-point bending specimen (see e.g. [18]) with a total length of 200 mm, a height of 50 or 60 mm and a thickness of 25-30 mm, with a crack length equal to half the specimen height. The initial crack was created using a band saw and the last 2 mm's of crack (the tip) was formed by cutting with a razor blade. The testing was performed in standard universal testing machine under quasi-static conditions (prescribed displacement rate of 1 mm/minute) and the value of K_{1c} was extracted using the load at onset of crack propagation, which in all cases appeared to

be unstable. The values of the fracture toughness are also included in Table 1 and they also seem to scale well with the relative density to the power or 1.1.

Crack propagation rate testing

In [13] crack propagation tests of Divinycell H100 and Rohacell WF51 were performed using a compact tension (CT) specimen [18], as illustrated in Fig.3. The dimensions was scaled up considerably compared to a standard metallic specimen using a characteristic length W = 225 mm. The same specimen type was again used to extract crack propagation data for the other qualities studied herein. The test is thus performed to obtain crack propagation data in the plane of the material block.

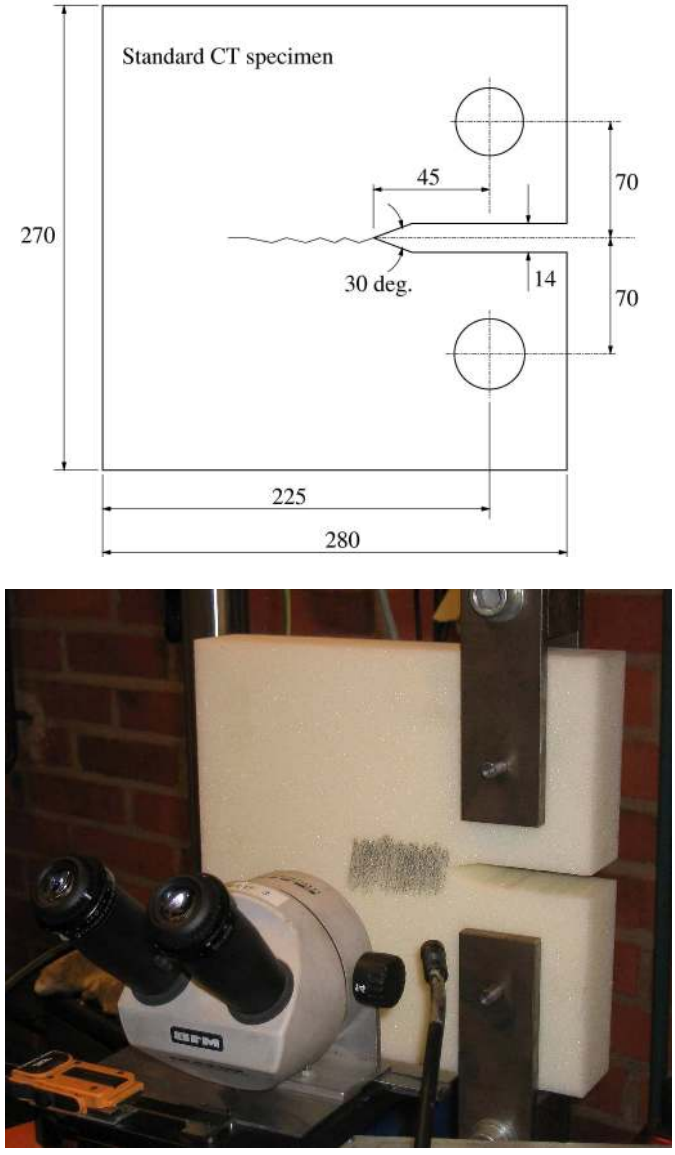

Figure 3 Geometry and photograh of the CT specimen

The specimens were tested using a sinusoidal load in load control at 2 Hz at a load ratio R = 0.1. The crack length was monitored using a travelling microscope and measured on one surface only. Tests were done by injecting paint into the crack front, then propagating the crack some distance (several millimetres) and cracking the specimen open. It was found that

the crack remains straight through the thickness of the specimen and thus one-sided measurements should be ample. Several crack length readings were done on each specimen and the load was shed (decreasing the load) in order to vary the stress intensity range, but keeping the stress ratio constant.
The crack propagation measurements were fitted using Paris' law

$$\frac{da}{dN} = C\Delta K_I^m \text{ where } da/dN \text{ is given in mm/cycles} \quad (2)$$

Where da/dN is the crack propagation rate, ΔK_I is the stress intensity range, m is the slope of the relation in a log-log scale and C is a constant. For details on the data reduction, see [13]. The Paris' law curves for the three densities of Divinycell and Rohacell are shown in Fig.4. The slope has been found by combining all results from one group of materials (H-grade or WF-grade) and finding a common slope for all densities using a standard linear curve fit. Curve fits to the individual data sets results in almost the same slope, but with some small variation. In doing one obtains the Paris' law constants C presented in Table 1.

(a) (b)

Figure 4 (a) da/dN vs. ΔK curves for Divinycell H60, H100 and H200 (left to right) and (b) for Rohacell WF51, WF110 and WF200 (left to right)

There are a few important conclusions from these test results; the crack growth rates are very high; m = 6 for Divinycell H and m = 13 for Rohacell WF. Actually, very high Paris law exponents were reported on Aluminium foams [12], as high as up to m = 25, although the base material of the foam was aluminium which in its bulk form has a Paris law exponent in the order of 2-4. We can further conclude that the slope m in the Paris' law data appears to be

the same for each material grade, irrespective of density, of course within some experimental scatter. For practical purposes this means crack grows very fast once they start growing and the stress intensity range of stable crack growth is thus narrow.

Upon noting that the stress intensity is proportional to the applied stress (or load) and that in fact the strength and fracture toughness scales with relative density to the same power (1.1 in this case), we could assume that the crack growth rate scales the same way (being proportional to the stress intensity). This type of scaling with relative density was first done by Huang and Lin [15] for phenolic foams of varying density. By taking the data in Fig.4 we can normalise ΔK with the relative density using $\Delta K/\rho^n$ and if this is done to all Paris' law curves collide into one single relation, as shown in Fig.5.

(a) (b)

Figure 5 (a) da/dN vs. $\Delta K/\rho^n$ curves for Divinycell H60, H100 and H200 (left to right) and (b) for Rohacell WF51, WF110 and WF200

As seen in Fig.5, the Paris' law relation also appears be generic for a class of foams. There is a little mismatch in the data for WF110, which appears to a higher Paris law constant C than expected. The reason for this is unresolved. In short, this implies that once the property – relative density relation is known, one test should be ample to determine the properties for all densities of the same material. To create one master curve for all *da*/*dN* data could take the slope in Fig.5 and the corresponding number for C in the normalized graph. Normalising eq.(2) yields

$$\frac{da}{dN} = C\overline{\rho}^{n\times m}\left(\frac{\Delta K_I}{\overline{\rho}^n}\right)^m \quad \text{where } \overline{C} = C\overline{\rho}^{n\times m} \tag{3}$$

This can then be extracted for all relative densities and used for predictions. In the Rohacell case this approach may be a little dubious due to the high value of *m* since a small change in the relative density implies a large change in the Paris law constant *C*. In any case, the density normalized value of $\overline{C} = C\overline{\rho}^{n \times m}$ is also given in Table 1 and is as seen a fairly similar value for the different densities of the foam grade.

Tension-tension fatigue testing

The fatigue test procedure used an axi-symmetric dog bone specimen, described in ASTM D1623-78 "Tensile and tensile adhesion properties of rigid cellular plastics" [19]. The specimens were cut from blocks of foam core, bonded between two aluminium cylinders and a waist was milled to the correct shape and size in a lathe. Thus, this testing is done in the thickness direction of the foam material block. The test rig with a specimen is shown in Fig.6.

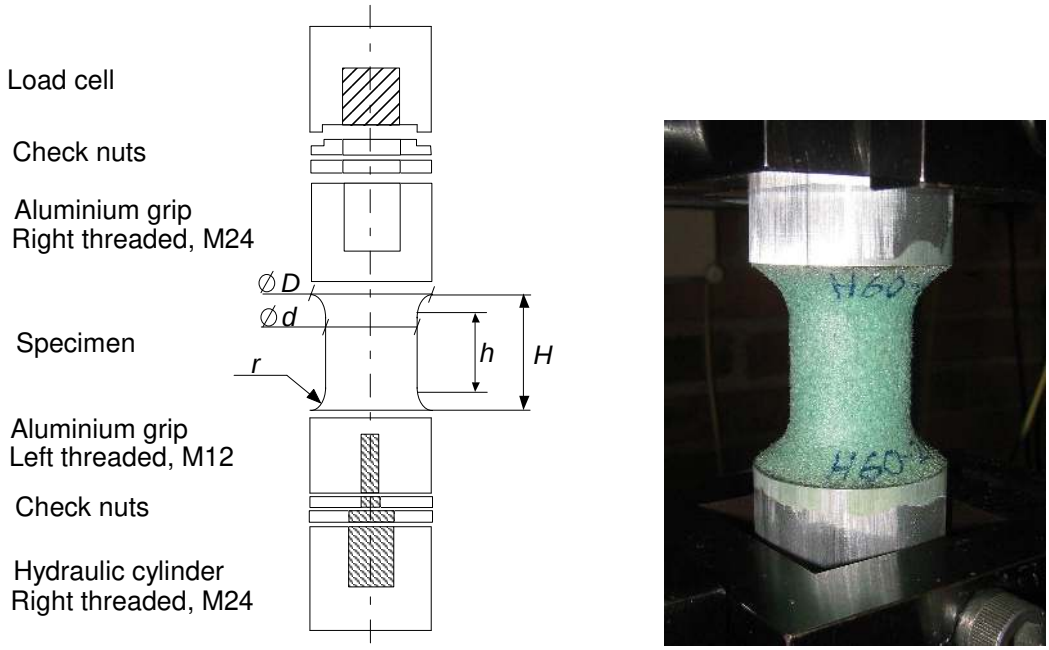

Figure 6 (a) Schematic drawing of the test set-up tensile fatigue specimen. Dimension used *D* = 50 mm, *d* = 30 mm, *H* = 50 mm, and *h* = 32 mm. (b) Photograph of H60 speciment mounted in the testing machine.

Static tests were performed in tension under a constant deformation rate of 2 mm/min at room temperature using the same specimen type. The fatigue tests were performed under a load controlled sinusoidal cycle using a servo hydraulic testing machine. The load ratio used was in all cases $R = 0.1$, $R = \sigma_{min}/\sigma_{max}$ and a testing frequency of 5 Hz. The fatigue life of the specimens is characterised as the number of cycles to ultimate failure.

There were no visual signs of damage in the specimens prior to failure, which occurred abruptly. Monitoring the stiffness of the specimens throughout the testing exhibited no measurable changes in stiffness up until the final load cycles prior to complete rupture.

Stress-life and Paris' law correlation

Huang and Lin [15] analysed crack propagation data of various density phenolic foams reported in [1]. Their modelling of crack growth rates is based on the assumption that incremental crack growth is governed by the rupture of individual cell implying that the

models include the characteristic length scale of the cell size. In doing this, they use a Basquin's law type S-N relation for the solid material in the cell edges and via dimensional analysis based on the open cell models in [1] derive an expression for the Paris' law relation. This relation implies that the relative density scaling, based on open cell foams, must be 1.5. In realising this Huang and Lin are able to normalise the Paris' law data to one single generic relation for all density phenolic foams. However, the parameters in the derived Paris' law expression remains unknown.

The model for fracture toughness of open cell foams given in [1], which is used in [15] involves a length scale implying that the fracture toughness should scale with the square root of the cell size. The same scaling appears if one does a similar model for closed cell foams. This effect does not exist in the tested material. The argument behind this statement stems from testing of Divinycell H60 with different cell size. The materials tested had the same density and made from the same solid material. But, the cell size varied more than one order of magnitude (from approximately 0.2 mm to 4 mm in cell diameter). These materials all had the same tensile characteristics (modulus, strength, etc.) and also the same mode I fracture toughness.

Herein, we assume crack growth in the closed cell polymer foam to be continuous, as in a continuum. The approach to find a link between the stress-life or often called S-N curve and the crack growth measurements is then similar to that of homogeneous materials. The approach is thus the opposite to that used by Huang and Lin [15]. We assume the fatigue life to be a crack growth test from some *initial flaw size* a_0 to a final crack size a_f. The initial flaw size is then considered to be some typical defect present in the volume of the material. The final crack size, a_f, is simply some defect size in the test specimen that will fracture the specimen in one single load cycle and is thus linked to the fracture toughness of the material. Starting from Paris' law we have

$$\frac{da}{dN} = C\Delta K_I^m = C\left(\Delta\sigma_0\sqrt{\pi a}\cdot f\right)^m = C\Delta\sigma_0^m(\pi a)^{m/2}\cdot f^m \tag{4}$$

with experimentally known coefficients and where f is a function that depends on the geometry of the specimen, the crack shape and the crack length. By integrating eq.(4) the number of cycles required to propagate a crack of some initial length a_0, usually denoted the *initial flaw size*, to a critical length a_f, that creates complete rupture of the specimen can be obtained. The critical length is simply given by some length that leads to static failure at peak load during a fatigue cycle. This is given by

$$a_f = \frac{1}{\pi}\left(\frac{K_{Ic}}{\Delta\sigma_{0,\max}\cdot f}\right)^2 = \frac{1}{\pi}\left(\frac{K_{Ic}(1-R)}{\Delta\sigma_0\cdot f}\right)^2 \tag{5}$$

If we assume a circular crack with radius a in a finite size cylinder of radius R, as illustrated in Fig.7, the finite width correction factor f equals [18]

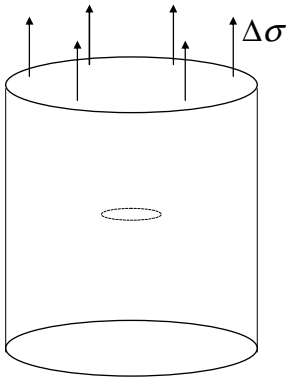

Figure 7 Schematic of cylindrical specimen with internal circular crack

$$f(a/R) = \frac{2}{\pi} \frac{1 - \frac{a}{2R} + 0.148\left(\frac{a}{R}\right)^3}{\sqrt{1-\frac{a}{R}}} \tag{6}$$

This finite width correction factor is seen to be close to its asymptotic value $2/\pi$ for ratios of the crack radius to specimen radius up to almost 0.3 (then $f = 1.011 \cdot 2/\pi$). If the initial flaw size is small compared to the critical size, most of the fatigue life will be governed by the growth of a small crack. This in turn means that the finite width correction factor will remain approximately constant for most of the load cycles and crack growth. Thus, we shall treat f as being a constant and for simplicity let's assume it to be unity, i.e., $f = 1$. Another implication of this is that one can assume stable growth of cracks in the specimen almost up until complete rupture of the specimen.

Anyhow, assuming these conditions to be approximately satisfied, the number of cycles to failure can obtained by integration of eq.(4)

$$\int_0^{N_f} dN = \int_{a_0}^{a_f} \frac{da}{C\Delta\sigma_0^m (\pi a)^{m/2}} \tag{7}$$

The number of load cycles to failure, N_f, is then given by

$$N_f = \frac{1}{C\Delta\sigma_0^m (\pi)^{m/2}} \int_{a_0}^{a_f} (a)^{-m/2}\, da = \frac{1}{C\Delta\sigma_0^m (\pi)^{m/2}} \left(\frac{(a_f)^{1-m/2} - (a_0)^{1-m/2}}{1-m/2} \right) \tag{8}$$

Let us also first for simplicity assume that the critical crack size is much larger than the initial one, so that the fatigue life of a small specimen is the same as for a large one. The reason being that the exponent in Paris' law is quite high. If so, the number of cycles to failure will be

$$N_f \approx \frac{1}{C\Delta\sigma_0^m (\pi)^{m/2}} \left(\frac{(a_0)^{1-m/2}}{m/2-1} \right) \tag{9}$$

This can now be rewritten to a Basquin's law type equation

$$\Delta\sigma_0 \approx \frac{(a_0)^{1/m-1/2}}{C^{1/m}\sqrt{\pi}}(m/2-1)^{-1/m} N_f{}^{-1/m} \tag{10}$$

or

$$\sigma_{0,\max} \approx \frac{(1-R)(a_0)^{1/m-1/2}}{C^{1/m}\sqrt{\pi}}(m/2-1)^{-1/m} N_f{}^{-1/m} \tag{11}$$

where $\sigma_{0,\max}$ is the maximum stress in the load cycle. The slope of this curve is $-1/m$ and is thus linked to the slope of the Paris' law curve. This equation has limited validity, i.e., we go from high-cycle fatigue described by Basquin's law, to low-cycle fatigue when the maximum applied stress exceeds the yield strength, here defined as $\sigma_{0.2}$. This occurs when

$$N_{f,\lim it} \approx \frac{(1-R)^m}{C\sigma_{0.2}^m(\pi)^{m/2}}\left(\frac{(a_0)^{1-m/2}}{m/2-1}\right) \tag{12}$$

Now we run into some problems since both $N_{f,\text{limit}}$ and a_0 are unknown. The way to proceed proposed in here is to perform at least one tension-tension fatigue test at which $\Delta\sigma_{0,\max} = \sigma_{0.2}$ to get an estimate for $N_{f,\text{limit}}$. Once this number is established, the initial flaw size can be calculated. This is done by converting eq.(12) to

$$a_0 \approx N_f^{\frac{1}{1-m/2}}(m/2-1)^{\frac{1}{1-m/2}} C^{\frac{1}{1-m/2}} \Delta\sigma_0^{\frac{m}{1-m/2}} (\pi)^{\frac{m}{2(1-m/2)}} \tag{13}$$

We can get the initial flaw size by means of knowing the Paris' law constant C, the Paris' law exponent m and one point on the S-N curve. From this, we can actually construct a synthetic S-N curve based on a value of a_0. This S-N curve is then valid for cycle numbers in the high-cycle fatigue regime, i.e., down to $N_{f,limit}$.

Results and discussion

The results from the tension-tension fatigue testing of Divinycell H60, H100 and H200 are presented in Fig.8 in double logarithmic scale as stress vs. number of cycles to failure. The horizontal line corresponds to the yield stress ($\sigma_{0.2}$) of the material. In order to get the synthetic S-N curve for the material the following data has been used; firstly, the number of cycles to failure for the specimens tested at a maximum stress $\sigma_{\max} = \sigma_{0.2}$ has been used to find the number of cycles to failure at nominal yield stress. This can then be used via eq.(13) to find a value for the initial flaw size a_0. For Divinycell, the number of cycles to failure at yield stress is approximately 10000, as seen from Figs.8a, but this is a lower limit. This gives an initial flaw size in order of 0.18-0.22 mm, assuming the correction factor $f = 1$, by using eq.(13). For Rohacell the corresponding transition from low-cycle to high-cycle fatigue is 100 cycles as a conservative estimate and this gives an initial flaw size of approximately 0.3 mm. The calculated values of a_0 using eq.(13) are given in Table 1.

(a)

(b)

Figure 8 S-N curves for (a) H60, H100 and H200. (b) WF51, WF110 and WF200

Several conclusions can be drawn for the obtained results; the slope of the S-N curves for each material within a group appears to be almost the same, although there is experimental scatter. This slope is equal to the slope of the synthetic S-N curve being the inverse of the Paris law exponent. Furthermore, at a cyclic stress maximum equal to the yield stress of the material, the slope changes and the experimental scatter increases.

The (yield) strength and the fracture toughness scale with relative density to the power of 1.1. Normalised S-N curves are shown in Fig.9.

(a)

(b)

Figure 9 Density normalised S-N curves for (a) H60, H100 and H200. (b) (b) WF51, WF110 and WF200.

The relative density normalised S-N curves appear to collapse into one single master curve. So what is really the initial flaw size? Does it exist or is it a superficial parameter? One thing that is experimentally observed in the crack propagation tests (CT-specimens) is that

individual cell walls, even at some distance ahead of the crack tip, ruptures while the cell edges remain intact. One such case is shown in the Fig.10.

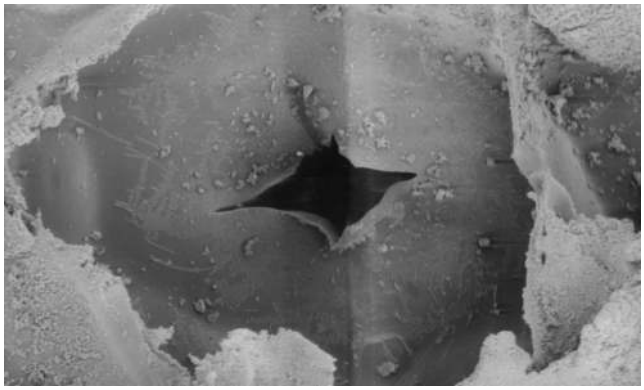

Figure 10 Photograph of cracked cell wall.

Although it is very hard to find any evidence of the process of fatigue crack nucleation and propagation in the un-notched specimen one can at least hypothesise around it. Going back to the models by Ashby and Gibson [1] the main hypothesis of deformation in foams is that cell edges bend and cell walls stretch. If that is the case then the local cell wall strain will be in the same order of magnitude as the global strain (will vary due to cell wall orientation to the loading direction). If cell edges bend then the bending strain in these edges will be smaller (actually proportional to the square root of the remote strain times the ratio of the cell edge thickness and its length). If this is the mode of deformation then one can assume that cell walls will rupture before the edges, creating an initial flaw with a size in the order of the cell size. This will most probably happen in many places in a volume of the foam and the process may then very well be similar to what has been noticed in fatigue of sandwich beams with foam cores [3] where it was found that micro-cracks in the foam nucleate in a zone of maximum stress. These micro-cracks then grow together to form a macroscopic crack. Once this large crack has formed it will then grow very fast and cause the test specimen to complete fracture within very few load cycles.

We can further relate the observations with that of aluminium foams [10] as discussed previously. In the testing performed in here, we find an accumulated (creep) strain as function of number of load cycles as shown in Fig.11.

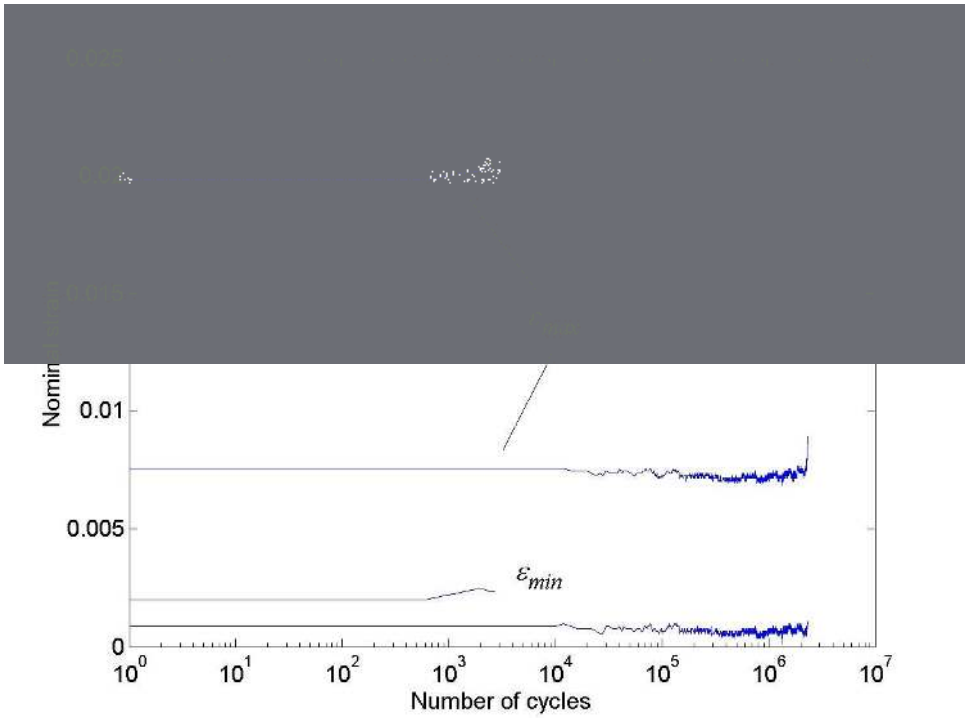

Figure 11 Accumulated strain in tension-tension fatigue of Divinycell H100 for specimens at two load levels; large and small number of cycles to failure.

As can be seen from Fig.11, there exists a small accumulated (creep) strain in the specimens run at high load level, with a small number of cycles to failure. In the specimens tested at low load level there is no evident creep present. For the Rohacell specimens the situation is similar. The highest creep strain found was smaller than 10% of the maximum applied strain. There is no evident knee in the strain-time plots as found in [10] for the entire life with the exception of the last few load cycles prior to complete failure. The small accumulated strain could be partially due to creep and partly due to cell wall cracking. By plotting the strain range in the load cycle (difference between maximum and minimum displacement in one cycle) as function of time reveals very little change in stiffness of the specimen, apart from the very last few load cycles. It is thus hard to draw any firm conclusions on the actual fatigue degradation process, be it accumulated local plastic strains in the cell walls and/or edges, or the formation of micro cracks in the cell walls that nucleate and slowly grow together. The latter seems more plausible from the observations done.

Another point of discussion is the results themselves and in the comparison between the two materials, one being brittle (Rohacell) and more ductile (Divinycell). If we go back to the results presented above we see that the yield stress (here defined as $\sigma_{0.2}$) is different in comparison to the ultimate strength; approximately $0.7\sigma_{ult}$ and $0.9\sigma_{ult}$ for Divinycell and Rohacell, respectively. This, in itself, may have some implications on the usage of these materials in the design process. Although these materials have quite different fatigue lives at yield stress (10^4 for Divinycell and 10^2 for Rohacell) we may actually also compare the fatigue lives at lower stress. Recall the difference in the slope of the S-N curve, which stems from the Paris' law exponent. This implies that at lower cyclic loads the situation changes. If we go back to the cylindrical specimen with an internal circular crack depicted in Fig.7 we can now actually predict the fatigue life at various stress levels. If we take, for example the maximum stress in the load cycle to be $\sigma_{0.2}/2$ we find that the fatigue life of Divinycell will be

approximately 10^6 cycles, whereas for Rohacell it will be closer to $5 \cdot 10^6$, i.e., a longer life. This is due to the lower slope of the S-N curve for the more brittle material. Recall also that a stress level $\sigma_{0.2}/2$ is equivalent to approximately $0.35\sigma_{ult}$ for Divinycell and $0.5\sigma_{ult}$ for Rohacell, i.e., a relatively higher stress compared to the static ultimate.
Another discussion issue is on the fatigue crack growth rates in general. The Paris' law exponents are high, considerably higher than for most homogeneous material, despite the fact the some foams appear to behave like fairly ductile materials on a macroscopic scale. However, any kind of imperfections in the material in terms of stress risers, cracks, notches, etc., could potentially have a severe effect on the fatigue performance since if a damage starts to grow, it will grow very rapidly.
As seen from the results, crack growth rates have been measured down to 10^{-6} mm/cycle without any indications of a fatigue threshold. Assuming we have such low rates present in the material implies that these foams will exhibit fatigue degradation (stable crack growth) in the order of 10^7 load cycles, at least. Any fatigue endurance limit, if it exists, will then be above this value, being practically very hard to find.

Conclusions and future work

The main aim with this investigation was to use Paris' law data to predict the fatigue life of foams under tension loading. Paris law data for the foams were used together with one tension-tension fatigue test to predict the S-N curve for the foam. The correlation between this prediction and the experimental obtained fatigue data is quite satisfactory. It is further seen that static properties of a certain class of foams can be normalised with the relative density and a unique, density independent property can be obtained. The same normalisation can also be performed on Paris law relations and fatigue data. The conclusion of this is that the fatigue life in tension for one class of foams appears to be possible to predict using one (or perhaps a few) tension-tension fatigue tests at e.g. yield stress together with crack propagation data. These tests are both fairly fast and cheap to perform. Fatigue data can then be predicted for other densities using relative density normalisation.
The long-term aim of this project is to be able to predict the fatigue life of foams, under general loading conditions, without the need for extensive testing. This could be particularly important in the design process of foam core sandwich structures. Secondly, gaining certainty into issues like fatigue, safety factors could potentially be decreased thus saving structural weight.

Acknowledgements

The financial support for this investigation has been provided by The Office of Naval Research (ONR) through programme officer Dr. Yapa D.S. Rajapakse (Grant No. N00014-99-1-0316). DIAB Sweden and Röhm GmbH are also acknowledged for supplying the materials. Special thanks to Anders Bäckman for performing the major parts of the tension-tension fatigue testing.

References

[1] Gibson L.J. and Ashby M.F., *Cellular Solids – Structure and Properties*, 2:nd edition, Cambridge University Press, Cambridge, UK, 1997.

[2] Burman, M., *Fatigue Crack Initiation and Propagation in Sandwich Structures*, Ph.D. Disseration, Dept. of Aeronautics, Kungliga Tekniska Högskolan, chapter 8, report 98-29, 1998.

[3] Burman M. and Zenkert D., "Fatigue of Foam Core Sandwich Beams, Part I: Undamaged Specimens", *International Journal of Fatigue*, Vol, 19, No 7, 1997, pp 551-561.

[4] Burman M. and Zenkert D., "Fatigue of Foam Core Sandwich Beams, Part II: Effect of Initial Damages", *International Journal of Fatigue*, Vol, 19, No 7, 1997, pp 563-578.

[5] Shenoi R.A., Clark S.D. and Allen H.G., "Fatigue Behaviour of Polymer Composite Sandwich Beams", *Journal of Composite Materials*, Vol.29, No.18, 1995, pp 2423-2445.

[6] Buene L., Echtermeyer A.T. and Sund O.E, "Fatigue Properties of PVC Foam Core Materials", *Det Norske Veritas Report 91-2049*, 1991.

[7] Kanny K. and Mahfuz H., "Flexural fatigue characteristics of sandwich structures at different loading rates", *Composite Structures*, Vol.67, No 4, 2005, pp 403-410.

[8] Kanny K., Mahfuz H., Carlsson L.A., Thomas T. and Jeelani S., "Dynamic mechanical analyses and flexural fatigue of PVC foams", *Composite Structures*, Vol.58, No 2, 2002, pp 175-183.

[9] Kulkarni N., Mahfuz H., Jeelani S. and Carlsson L.A., "Fatigue crack growth and life prediction of foam core sandwich composites under flexural loading", *Composite Structures*, Vol.59, No 4, 2003, pp 499-505.

[10] McCullough K.Y.G., Fleck N.A. and Ashby M.F., "The stress-life fatigue behaviour of aluminium alloy foams", *Fatigue and Fracture of Engineering Materials and Structures*, Vol.23(3), 2000, pp 199-208

[11] Harte A.-M., Fleck N.A. and Ashby M.F., "Fatigue Failure of an Open and a Closed Cell Aluminium Alloy Foam", *Acta Materialia.*, Vol 47, No 8, 1999, pp 2511-2524.

[12] Olurin O.B., McCullough K.Y.G., Fleck N.A. and Ashby M.F., "Fatigue Crack Propagation in Aluminium Alloy Foams", *International Journal of Fatigue*, Vol 23, No 5, 2001, pp 375-382.

[13] Shipsha A., Burman M. and Zenkert D., "On Mode I Fatigue Crack Growth in Foam Core Materials for Sandwich Structures", *Journal of Sandwich Structures and Materials*, Vol 2, No 2, 2000, pp 103-116.

[14] Shipsha A., Burman M. and Zenkert D., "Interfacial Fatigue Crack Growth in Foam Core Sandwich Structures", *Fatigue & Fracture of Engineering Materials & Structures*, Vol 22, No 2, 1999, pp 123-131.

[15] Huang J.S. and Lin J.Y., “Fatigue of Cellular Materials”, *Acta mater.*, Vol 44, No 1, 1996, pp 289-296

[16] *Divinycell H-grade, Technical Manual*, DIAB AB, Laholm, Sweden, www.diabgroup.com.

[17] *Rohacell WF*, Röhm Degussa-Hüls group, www.roehm.com

[18] Tada H., Paris, P. C. and Irwin G. R., *The Stress Analysis of Cracks Handbook*, 2nd Ed., Paris Production Inc., Missouri, USA, 1985

[19] *Annual Book of the ASTM Standards,* American Society for Testing and Materials, Philadelphia, PA.